Cancer Cell
Article

HIF-1 Inhibits Mitochondrial Biogenesis and Cellular Respiration in VHL-Deficient Renal Cell Carcinoma by Repression of C-MYC Activity

Huafeng Zhang,[1,2] Ping Gao,[3] Ryo Fukuda,[1,2] Ganesh Kumar,[5] Balaji Krishnamachary,[1,2] Karen I. Zeller,[3] Chi V. Dang,[3] and Gregg L. Semenza[1,2,3,4,*]
[1] Vascular Biology Program, Institute for Cell Engineering
[2] McKusick-Nathans Institute of Genetic Medicine
[3] Departments of Medicine and Oncology
[4] Departments of Pediatrics and Radiation Oncology
The Johns Hopkins University School of Medicine, Baltimore, MD 21205, USA
[5] Center for Systems Biology, Department of Medicine, University of Chicago, Chicago, IL 60637, USA
*Correspondence: gsemenza@jhmi.edu
DOI 10.1016/j.ccr.2007.04.001

SUMMARY

Many cancer cells are characterized by increased glycolysis and decreased respiration, even under aerobic conditions. The molecular mechanisms underlying this metabolic reprogramming are unclear. Here we show that hypoxia-inducible factor 1 (HIF-1) negatively regulates mitochondrial biogenesis and O_2 consumption in renal carcinoma cells lacking the von Hippel-Lindau tumor suppressor (VHL). HIF-1 mediates these effects by inhibiting C-MYC activity via two mechanisms. First, HIF-1 binds to and activates transcription of the *MXI1* gene, which encodes a repressor of C-MYC transcriptional activity. Second, HIF-1 promotes MXI-1-independent, proteasome-dependent degradation of C-MYC. We demonstrate that transcription of the gene encoding the coactivator PGC-1β is C-MYC dependent and that loss of PGC-1β expression is a major factor contributing to reduced respiration in VHL-deficient renal carcinoma cells.

INTRODUCTION

The efficiency with which mitochondria synthesize ATP through oxidative phosphorylation is critical for the generation and maintenance of the structural and functional complexity that characterizes multicellular organisms. Energy generation is required for cell survival, but the mitochondria also generate reactive oxygen species (ROS) that can oxidize nucleic acids and proteins, resulting in cell dysfunction or death. In the presence of O_2, nontransformed cells convert glucose to pyruvate, which enters mitochondria, is converted to acetyl coenzyme A, and metabolized via the tricarboxylic acid cycle, yielding reducing equivalents that are used for oxidative phosphorylation to generate ATP. Under hypoxic conditions, lactate dehydrogenase A (LDH-A) catalyzes conversion of pyruvate to lactate. A characteristic feature of cancer cells is their increased metabolism of glucose to lactate even under aerobic conditions (the Warburg effect). Warburg proposed that respiration was impaired in cancer cells leading to increased glycolytic metabolism (Warburg, 1930). The increase in glucose uptake is such a reliable feature of cancer cells that it provides the basis for clinical identification of occult metastases by [^{18}F]-deoxyglucose positron-emission tomography (Gatenby and Gillies, 2004).

SIGNIFICANCE

In the presence of O_2, cells convert glucose to pyruvate, which enters the mitochondria and is metabolized, yielding reducing equivalents that are used for oxidative phosphorylation to generate ATP. Under hypoxic conditions, pyruvate is shunted away from the mitochondria by conversion to lactate. Cancer cells are characterized by increased glucose uptake, increased lactate production, and decreased respiration, even under aerobic conditions. The molecular mechanisms underlying this metabolic reprogramming of cancer cells are unclear. Loss of function of the von Hippel-Lindau tumor suppressor protein in renal cell carcinoma leads to dramatically reduced mitochondrial mass and O_2 consumption. We delineate a transcriptional network controlled by hypoxia-inducible factor 1 that is responsible for the dramatic decrease in respiration observed in renal carcinoma cells.

Studies of Rous sarcoma virus-transformed cells demonstrated that one of the earliest effects of *v-src* expression was an increase in glucose uptake and lactate production (Carroll et al., 1978). Inhibition of LDH-A activity impairs tumor cell proliferation ex vivo and in vivo (Shim et al., 1997; Fantin et al., 2006). Expression of two other glycolytic enzymes, phosphoglycerate mutase and glucose phosphate isomerase, was shown to immortalize primary human cells and attenuate the mitochondrial generation of ROS, which are known to cause cellular senescence (Kondoh et al., 2005).

The increased transcription of genes encoding glucose transporters and glycolytic enzymes, including LDH-A, in response to intratumoral hypoxia, V-SRC, and other oncoproteins is mediated by hypoxia-inducible factor 1 (HIF-1) (Semenza et al., 1994, 1996; Firth et al., 1995; Jiang et al., 1997; Iyer et al., 1998; Seagroves et al., 2001; Robey et al., 2005). Other transcription factors, including C-MYC (Shim et al., 1997; Osthus et al., 2000) and SP1/SP3 (Discher et al., 1998), contribute to the regulated expression of these genes. Glucose transport and aerobic glycolysis are also stimulated by oncogenic alterations that increase AKT kinase activity (Elstrom et al., 2004).

Several different transcription factors have been shown to regulate mitochondrial biogenesis, including mitochondrial transcription factors A (TFAM) and B (TFB1M, TFB2M), nuclear respiratory factor 1 (NRF-1), GA binding proteins (GABPα, GABPβ2), peroxisome proliferator-activated receptors (PPAR-α, PPAR-γ), PPAR-γ coactivators (PGC-1α, PGC-1β), PGC-1-related coactivator 1 (PPRC1), and C-MYC (Kelly and Scarpulla, 2004; Bogacka et al., 2005; Li et al., 2005). Somatic mutations have been identified in the mitochondrial genome of cancer cells (Polyak et al., 1998) and shown to promote tumor growth in xenograft assays (Petros et al., 2005). Cellular content and activity of mitochondria are reduced (Cuezva et al., 2002, 2004), lactate production is increased (Brizel et al., 2001) in many cancers, and these metabolic alterations are associated with poor prognosis. However, the molecular pathways underlying these observations have not been fully delineated.

In the majority of cases of renal clear cell carcinoma, activity of the von Hippel-Lindau tumor suppressor (VHL) protein is lost as a result of genetic or epigenetic changes in the cancer cell genome (Garcia, 2006). VHL loss of function, which leads to HIF-1 gain of function, is the earliest detectable molecular event in the pathogenesis of this cancer (Mandriota et al., 2002). HIF-1 is required for tumorigenesis in VHL-deficient renal carcinoma cells (Kondo et al., 2002; Maranchie et al., 2002). HIF-1 is a heterodimer composed of a constitutively expressed HIF-1β subunit and an O_2-regulated HIF-1α or HIF-2α subunit (Wang et al., 1995; Tian et al., 1997). HIF-1 has been shown to play critical roles in tumor angiogenesis, glucose metabolism, invasion/metastasis, and response to radiation and chemotherapy (Semenza, 2003; Tang et al., 2004; Moeller et al., 2005; Thomas et al., 2006 Esteban et al., 2006; Krishnamachary et al., 2006; Melillo, 2006). VHL binds to HIF-1α or HIF-2α and targets the protein for ubiquitination and proteasomal degradation in an O_2-dependent manner (Maxwell et al., 1999). VHL also has important functions that are not HIF-1-dependent, such as the regulation of p53 activity (Roe et al., 2006).

Reduced levels of mitochondrial DNA and respiratory chain proteins as well as increased levels of glycolytic enzymes have been reported in renal cell carcinoma (Simonnet et al., 2002; Unwin et al., 2003; Meierhofer et al., 2004; Craven et al., 2006). Forced expression of wild-type VHL protein in cell lines derived from VHL-deficient renal carcinoma leads to increased mitochondrial electron transport complex activity and increased levels of mitochondrial DNA and respiratory chain proteins (Hervouet et al., 2005), but the molecular pathways leading to these alterations have not been delineated (Hervouet and Godinot, 2006). In addition to its role in promoting glucose uptake and glycolysis, HIF-1 was recently shown to inhibit the metabolism of pyruvate to acetyl CoA in the mitochondria under hypoxic conditions by transactivation of the *PDK1* gene encoding pyruvate dehydrogenase kinase (Kim et al., 2006; Papandreou et al., 2006), suggesting that HIF-1 also regulates mitochondrial respiration. In this study, we tested the hypothesis that HIF-1 plays a broader role in the control of glucose and energy metabolism by negatively regulating mitochondrial biogenesis and O_2 consumption in renal carcinoma cells.

RESULTS

Mitochondrial Mass and O_2 Consumption Are Positively Regulated by VHL

We first sought to confirm a recent report that VHL loss of function is associated with a reduction in mitochondrial DNA content in renal carcinoma cells (Hervouet et al., 2005). RCC4 cells lack VHL activity and constitutively express HIF-1α and HIF-2α protein, whereas in the RCC4-VHL subclone, which is stably transfected with a VHL expression vector, the expression of HIF-1α and HIF-2α protein is induced only under hypoxic culture conditions (Figure 1A), as previously demonstrated (Maxwell et al., 1999; Hu et al., 2003; Krishnamachary et al., 2006). DNA extracted from cells cultured under nonhypoxic conditions was analyzed by quantitative real-time PCR to determine the ratio of mitochondrial:nuclear DNA. Stable transfection of a VHL expression vector into RCC4 cells resulted in a 2.5-fold increase in mitochondrial DNA content (Figure 1B).

To determine whether the reduction in mitochondrial DNA associated with VHL loss of function reflected a reduction in mitochondrial mass, cells were stained with nonyl acridine orange (NAO), a metachromatic dye that binds to cardiolipin in mitochondria regardless of their energetic state or membrane potential. Compared to RCC4-VHL cells, the distribution of mitochondrial mass in RCC4 cells was shifted toward reduced mitochondrial mass (Figure 1C). The 2.5-fold reduction in mitochondrial mass was associated with a >2.5-fold reduction in O_2 consumption by RCC4 as compared to RCC4-VHL cells (Figure 1D and 1E). Measurement of electron transport complex III

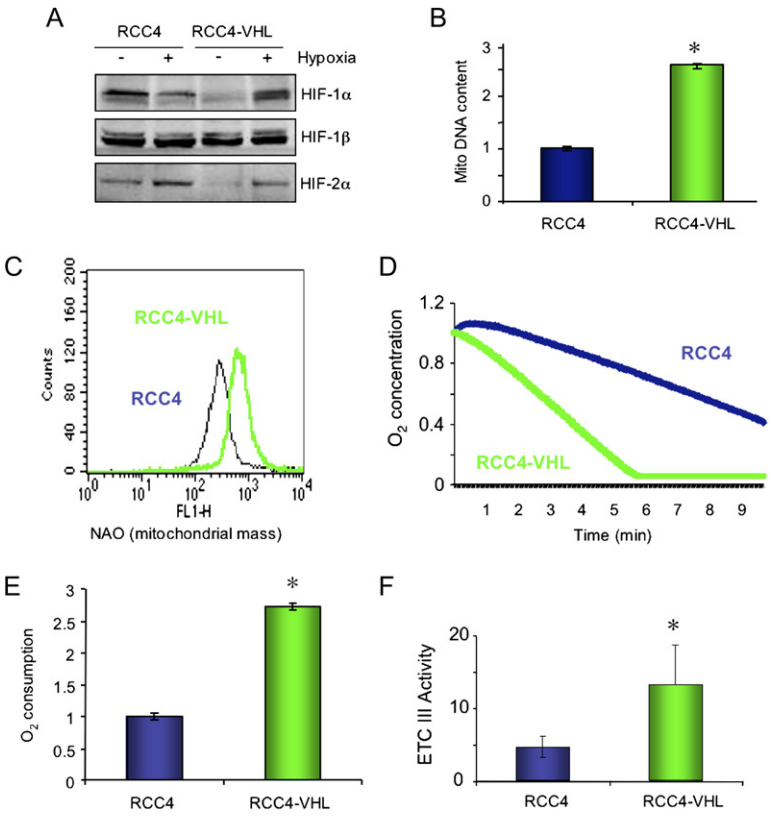

Figure 1. Analysis of VHL-Deficient and VHL-Rescued RCC4 Subclones

(A) The expression of HIF-1 subunit proteins under nonhypoxic (−) or hypoxic (+) conditions was determined by immunoblot assay of VHL-deficient parental RCC4 cells and a subclone that was stably transfected with a VHL expression vector (RCC4-VHL).

(B) The ratio of mitochondrial:nuclear DNA was determined by real-time PCR in RCC4-VHL cells and normalized to the result obtained from RCC4 cells.

(C) Equal numbers of RCC4 and RCC4-VHL cells were stained with NAO and analyzed by flow cytometry to measure mitochondrial mass.

(D and E) RCC4 subclones were incubated with a Clark-type electrode to measure O_2 concentration as a function of time (D) and to calculate rates of O_2 consumption (E).

(F) Electron transport complex (ETC) III activity was determined in isolated mitochondria.

*Mean (±SEM) that is significantly different from RCC4 ($p < 0.05$ by Student's t test).

activity in isolated mitochondria revealed a 2.8-fold difference between RCC4 and RCC4-VHL cells (Figure 1F).

RCC10 is an independently derived VHL-deficient renal carcinoma cell line (Krieg et al., 2000; Esteban et al., 2006) in which HIF-1α and HIF-2α are also overexpressed, resulting in increased expression of HIF-1 target genes (Figure S1 in the Supplemental Data available with this article online). RCC10 cells also showed reduced mitochondrial DNA content, mitochondrial mass, and O_2 consumption as compared to RCC10-VHL, a subclone that is stably transfected with a VHL expression vector (Figure S2).

Mitochondrial Mass and O_2 Consumption Are Negatively Regulated by HIF-1

To determine whether HIF-1 gain of function played a role in the reduced mitochondrial mass and O_2 consumption that was associated with VHL loss of function, RCC4 cells were stably transfected with an expression vector encoding HIF-1αDN, a dominant-negative form of HIF-1α that forms heterodimers with HIF-1β that cannot bind to DNA (Jiang et al., 1996), thus inhibiting the expression of HIF-1 target genes (Figure S3). Mitochondrial DNA content (Figure 2A), mitochondrial mass (Figure 2B), and O_2 consumption (Figure 2C) were all increased in the RCC4-DN subclone as compared to the parental RCC4 cells. These data indicate that HIF-1 transcriptional activity is necessary for the reduced mitochondrial content and O_2 consumption associated with VHL loss of function.

HIF-1αDN competes with both HIF-1α and HIF-2α for dimerization with HIF-1β. HIF-1 heterodimers containing HIF-1α or HIF-2α regulate an overlapping but distinct set of transcriptional target genes (Hu et al., 2003; Raval et al., 2005). To determine whether HIF-1α was specifically required for the loss of mitochondrial metabolism in RCC4 cells, we analyzed subclones stably transfected with an empty vector (RCC4-EV) or vector encoding a short hairpin RNA (shRNA) that specifically targets HIF-1α mRNA for degradation (RCC4-sh1). RCC4-sh1 cells expressed reduced levels of HIF-1α protein under nonhypoxic and hypoxic conditions, whereas the expression of HIF-1β and HIF-2α was unaffected (Figure 2D). Reduced HIF-1α expression resulted in a partial restoration of mitochondrial DNA content (Figure 2E) and O_2 consumption (Figure 2F) in RCC4-sh1 as compared to RCC4-EV cells.

We also analyzed stably transfected subclones expressing an shRNA that specifically targets HIF-2α mRNA for degradation (RCC4-sh2 pools P1 and P4). The HIF-2α protein level was inversely correlated with the mitochondrial DNA content and rate of O_2 consumption in these pools (Figure 2G, H). Thus, both HIF-1α and HIF-2α contribute to the negative regulation of mitochondrial metabolism in RCC4 cells.

The VHL/HIF-1 Pathway Regulates C-MYC Transcriptional Activity

Recently, C-MYC was shown to promote mitochondrial biogenesis (Li et al., 2005). To test the hypothesis that HIF-1 negatively regulates C-MYC activity in RCC4 cells, we performed quantitative real-time reverse transcription PCR (qrtPCR) to analyze the expression of two known

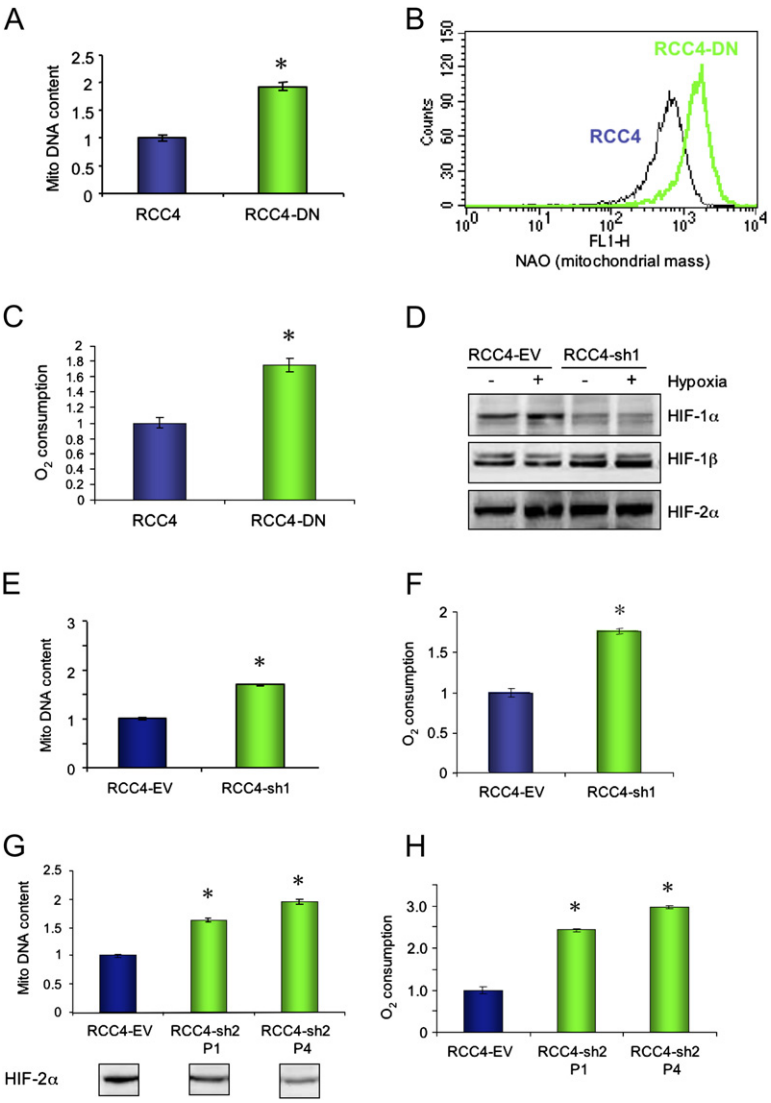

Figure 2. Effect of HIF-1 Loss of Function on Mitochondrial Metabolism

Mitochondrial DNA content, mitochondrial mass, and O_2 consumption were measured in RCC4 cells and subclones expressing HIF-1αDN, a dominant negative form of HIF-1α (A–C); short hairpin RNA directed against HIF-1α (D–F); or short hairpin RNA directed against HIF-2α ([G] and [H]; inset shows HIF-2α protein levels). *Mean (±SEM) that is significantly different from RCC4 or RCC4-EV.

C-MYC target genes, *CAD* and *RCL* (Boyd and Farnham, 1997; Lewis et al., 1997). In RCC4-VHL cells, expression of CAD (Figure S4A) and RCL (Figure S4C) mRNA was higher under nonhypoxic than under hypoxic conditions, whereas in VHL-deficient RCC4 cells, mRNA levels were not O_2-regulated and were similar to the levels in hypoxic RCC4-VHL cells. VHL-dependent CAD and RCL mRNA expression was also observed in RCC10 subclones (Figure S5). In VHL-deficient RCC4-sh1 cells, which express shRNA against HIF-1α, expression of the C-MYC target genes *CAD* (Figure S4B) and *RCL* (Figure S4D) was increased.

C-MYC Regulates Mitochondrial Mass and O_2 Consumption

To test the hypothesis that downregulation of C-MYC transcriptional activity contributes to the reduction of mitochondrial mass in RCC4 cells, a loss-of-function strategy was employed. RCC4 and RCC4-VHL cells were transfected with a pool of four short interfering RNAs (siRNAs), which target C-MYC mRNA for degradation, or a control RISC-free siRNA. The siRNAs eliminated the expression of C-MYC protein without affecting β-actin expression (Figure 3A) and decreased CAD and RCL mRNA expression (Figure S6A). In RCC4 cells, transfection of C-MYC siRNA did not affect mitochondrial DNA content (Figure 3B, compare lanes 1 and 3). However, in RCC4-VHL cells, which have high C-MYC levels, C-MYC siRNA significantly reduced mitochondrial DNA content (Figure 3B, lanes 2 and 4). C-MYC siRNA also reduced mitochondrial mass, as determined by NAO staining (Figure 3C), and O_2 consumption (Figure 3D) in RCC4-VHL cells to levels similar to those observed in RCC4 cells. In contrast, transfection of RISC-free control siRNA had no effect on C-MYC expression or mitochondrial mass.

In a complementary gain-of-function strategy, RCC4 and RCC4-VHL cells were transfected with expression vector encoding C-MYC, which resulted in increased

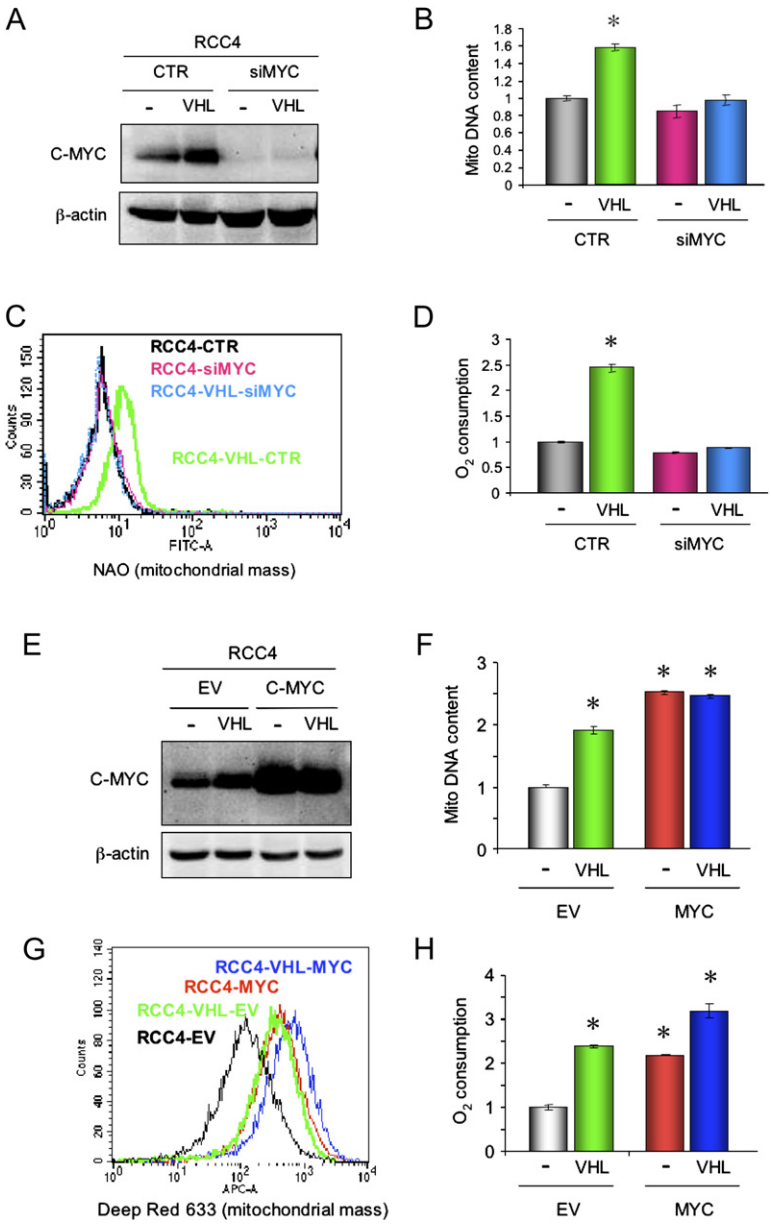

Figure 3. Effect of C-MYC Loss and Gain of Function on Mitochondrial Metabolism

(A–D) C-MYC loss of function. VHL-deficient and VHL-rescued RCC4 subclones were transfected with a control siRNA (CTR) or siRNA targeting C-MYC (siMYC) and analyzed for C-MYC protein expression (A), mitochondrial DNA content (B), mitochondrial mass (C), and O_2 consumption (D). *Mean (±SEM) that is significantly different from RCC4.

(E–H) C-MYC gain of function. RCC4 and RCC4-VHL cells were transfected with a retrovirus encoding C-MYC or an empty vector (EV) and analyzed for C-MYC protein expression (E), mitochondrial DNA content (F), mitochondrial mass by Deep Red 633 staining (G), and O_2 consumption (H). *Mean (±SEM) that is significantly different from RCC4-CTR or RCC4-EV.

C-MYC levels (Figure 3E) and increased CAD and RCL mRNA expression (Figure S6B). C-MYC overexpression led to an increase in mitochondrial DNA content (Figure 3F), mitochondrial mass (Figure 3G), and O_2 consumption (Figure 3H) in RCC4 and RCC4-VHL cells. Taken together, the gain/loss-of-function studies demonstrate that the effect of the VHL/HIF-1 pathway on mitochondrial metabolism is mediated through regulation of C-MYC activity.

HIF-1 Controls MXI-1 Expression in RCC4 Cells

MXI-1 competes with C-MYC for dimerization with MAX. MYC:MAX heterodimers activate transcription of target genes, whereas DNA binding of MXI-1:MAX heterodimers leads to transcriptional repression. MXI-1 expression is induced by hypoxia in wild-type, but not in HIF-1β-deficient, mouse hepatoma cells (Corn et al., 2005) and in human endothelial cells exposed to hypoxia or to adenovirus encoding a constitutively-active form of HIF-1α (Manalo et al., 2005). In VHL null RCC4 cells, MXI-1 mRNA (Figure 4A) and protein (Figure 4B) levels were markedly increased relative to levels in the RCC4-VHL subclone. Similar results were obtained using RCC10 subclones (Figures S5 and S7). The differences in MXI-1 expression between RCC4 and RCC4-VHL were independent of C-MYC (Figure S8). Among the other known members of the MYC/MAX/MXI-1 family, only MAD3 showed increased mRNA levels in RCC4 relative to RCC4-VHL cells (Figure S9).

Expression of shRNA against HIF-1α reduced MXI-1 mRNA and protein levels in the RCC4-sh1 cells as compared to the RCC4-EV subclone (Figure S10). Expression

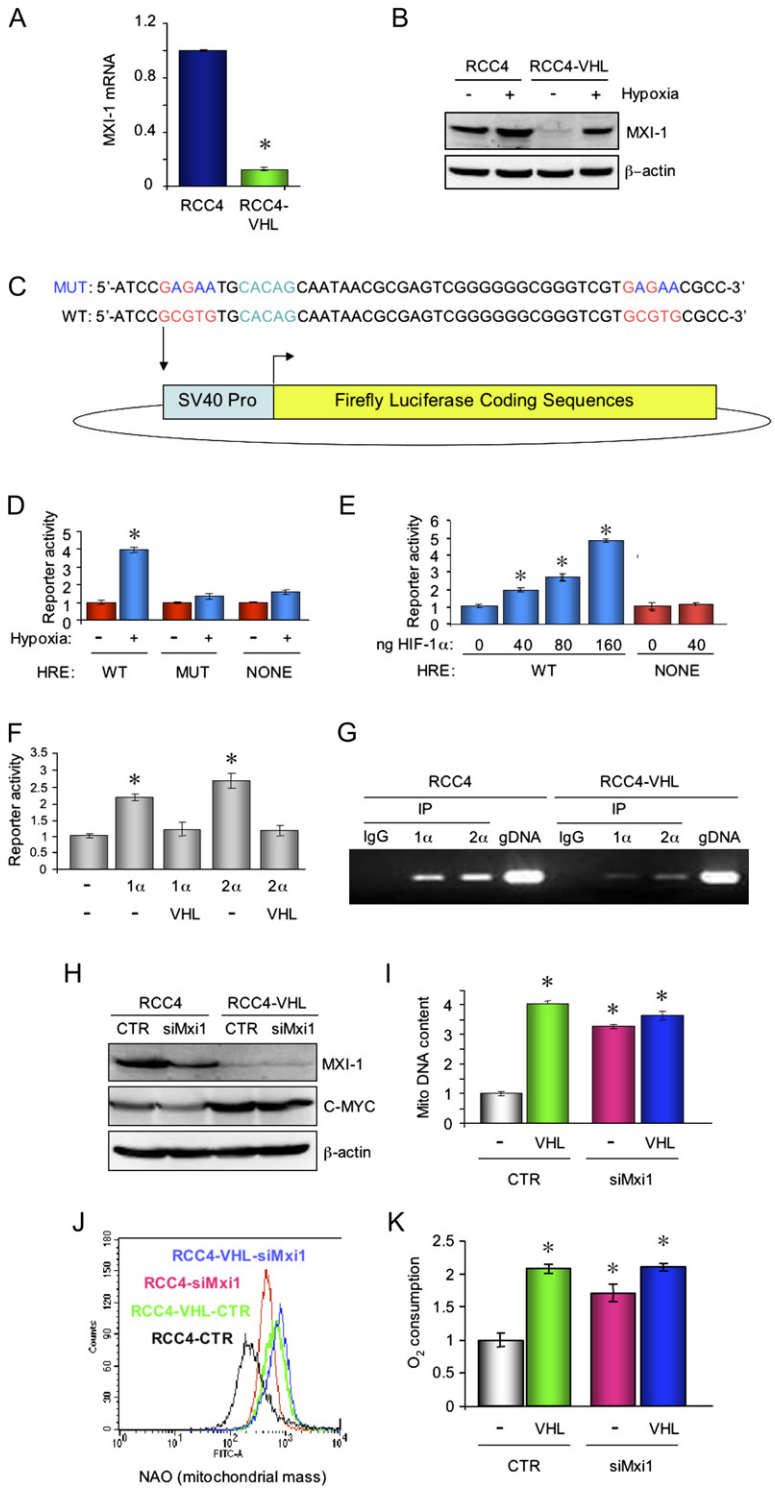

Figure 4. Analysis of MXI-1 Expression and Function in RCC4 and RCC4-VHL Cells

(A and B) Expression of MXI-1 mRNA (A) and protein (B) was determined in RCC4 subclones. β-actin was analyzed as a protein loading control. *Mean (±SEM) that is significantly different from RCC4.

(C) A 53-base-pair wild-type (WT) sequence from the human *MXI1* gene was identified that contains two copies of the consensus HIF-1 binding site 5′-RCGTG-3′ (red font) and one copy of the accessory sequence 5′-CACAG-3′ (green font). The putative hypoxia response element (HRE) sequence was amplified by PCR and inserted into a reporter plasmid, in which transcription of firefly luciferase coding sequences is driven by a basal promoter from the SV40 genome. A mutant sequence (MUT) containing nucleotide substitutions in the putative HIF-1 binding sites was also generated.

(D–F) 293 cells were transfected with a firefly luciferase reporter gene that contained WT, MUT, or no HRE. The cells were incubated under nonhypoxic or hypoxic conditions (D) or were cotransfected with HIF-1α, HIF-2α, or VHL expression vector (E and F) and incubated under nonhypoxic conditions for 24 hr. All cells were cotransfected with a control reporter expressing *Renilla* luciferase from the SV40 promoter. The ratio of firefly:*Renilla* luciferase was determined and normalized to the result obtained from cells incubated at 20% O_2 in the absence of HIF-1α. *Mean (±SEM) that is significantly different from control sample in first column of each panel.

(G) Chromatin from RCC4 or RCC4-VHL cells was subjected to immunoprecipitation (IP) with IgG or antibodies against HIF-1α or HIF-2α. DNA from the IP or genomic DNA (gDNA) was amplified by PCR using primers spanning the *MXI1* HRE.

(H–K) Cells were transfected with a control siRNA (CTR) or siRNA directed against MXI-1 (siMxi1) and assayed for MXI-1 protein by immunoblot assay (H), mitochondrial DNA content by real time PCR (I), mitochondrial mass by NAO staining and flow cytometry (J), and O_2 consumption using a Clark-type electrode (K). Results were normalized to those obtained from RCC4 cells transfected with CTR. *Mean (±SEM) that is significantly different from RCC4-CTR.

of shRNA against HIF-2α also reduced MXI-1 protein and mRNA levels in the RCC4-sh2 pools (Figure S11). Thus, both HIF-1α and HIF-2α contribute to *MXI1* gene expression in VHL-deficient renal carcinoma cells.

To demonstrate that *MXI1* is a direct target of HIF-1, we searched for a hypoxia response element (HRE). Known HREs consist of sequences of <70 bp that either contain a core HIF-1 binding site (5′-RCGTG-3′) followed after 1–8 bp by the sequence 5′-CACAG-3′ or contain multiple HIF-1 binding sites. We identified a sequence in the first intron of the human *MXI1* gene that fulfills these criteria and inserted it into a reporter plasmid in which luciferase coding sequences were driven by a minimal SV40 promoter (Figure 4C). Human 293 cells were transfected

with a reporter plasmid that contained the wild-type (WT) HRE, an HRE in which the HIF-1 sites were mutated (MUT), or no HRE. Luciferase activity was specifically increased in cells that were transfected with the WT reporter and cultured under hypoxic conditions (Figure 4D). Cotransfection of an expression vector encoding HIF-1α (Figure 4E-F) or HIF-2α (Figure 4F) increased WT reporter expression under nonhypoxic conditions. In contrast, VHL inhibited WT reporter expression induced by cotransfected HIF-1α or HIF-2α vector (Figure 4F). Mutation of the HIF-1 binding sites in the HRE resulted in loss of reporter gene response to hypoxia, HIF-1α, HIF-2α, or VHL (Figures 4C–4D; Figure S12). Chromatin immunoprecipitation (ChIP) assay demonstrated increased binding of HIF-1α and HIF-2α to the HRE in RCC4 cells as compared to RCC4-VHL cells (Figure 4G).

If HIF-1 inhibits mitochondrial metabolism by MXI-1-mediated repression of C-MYC, then MXI-1 loss of function should reverse the effects of VHL loss of function. Transfection of RCC4 cells with siRNA against MXI-1 lowered the levels of MXI-1 protein, although it remained elevated compared to RCC4-VHL cells (Figure 4H). MXI-1 loss of function was associated with recovery of mitochondrial DNA content, mitochondrial mass, and O_2 consumption (Figures 4I–4K).

HIF-1 Regulates C-MYC Protein Stability

Immunoblot assays revealed that C-MYC protein levels were regulated by VHL and O_2 in RCC4 cells (Figures 3A, 3E, 4H, and 5A). Expression of HIF-1αDN led to decreased MXI-1 and increased C-MYC protein levels (Figure 5B). Both HIF-1α and HIF-2α contributed to loss of C-MYC in RCC4 cells (Figures 5C and 5D). If the MXI-1-dependent inhibition of C-MYC dimerization with MAX led to C-MYC degradation, then MXI-1 knockdown should rescue C-MYC levels in RCC4 cells, but this was not observed (Figure 4H). The observed changes in C-MYC protein were not due to changes in C-MYC mRNA expression (Figure S13). However, the loss of C-MYC induced by hypoxia or VHL deficiency could be rescued by treatment with MG132 (Figures 5E and 5F), indicating that HIF-1 promotes C-MYC degradation through an MXI-1-independent, proteasome-dependent mechanism.

PGC-1β mRNA Expression Is Regulated by the VHL/HIF-1/C-MYC Pathway

To search for a factor that functions in the mitochondrial biogenesis pathway downstream of C-MYC, we performed qrtPCR to analyze the expression of mRNAs encoding mitochondrial RNA polymerase (POLRMT) and 11 transcription factors (GABPα, GABPβ2, NRF1, PPARα, PPARγ, PGC-1α, PGC-1β, PPRC1, TFAM, TFB1M, and TFB2M) that have been implicated in mitochondrial biogenesis (Kelly and Scarpulla, 2004; Bogacka et al., 2005; Uldry et al., 2006). Of these 12 mRNA species, only PGC-1β mRNA (Figure 6A and data not shown) and protein (Figure 6B) were increased in RCC4-VHL relative to RCC4 cells and therefore correlated with increased C-MYC activity and increased mitochondrial mass in

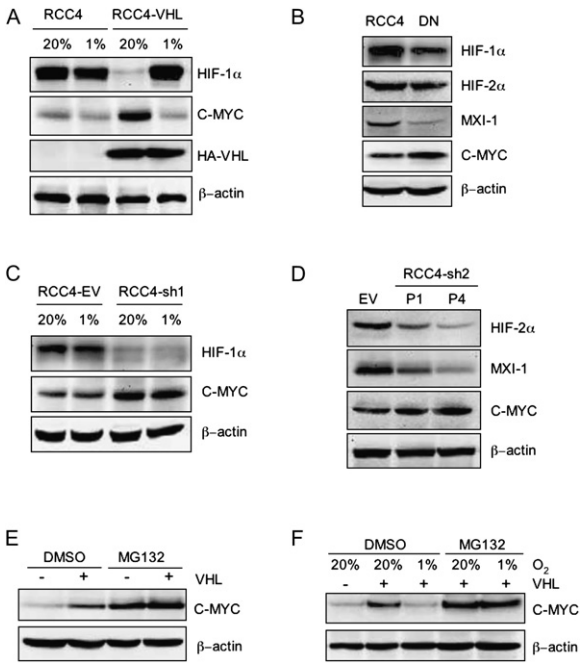

Figure 5. Regulation of C-MYC Protein Levels by HIF-1

(A–D) Immunoblot assays were performed with antibodies against the indicated proteins using lysates prepared from: RCC4 and RCC4-VHL cells that were incubated at 20% or 1% O_2 for 48 hr (A); nonhypoxic RCC4 and RCC4-DN cells (B); RCC4-EV and RCC4-sh1 cells that were incubated at 20% or 1% O_2 for 48 hr (C); and nonhypoxic RCC4-EV and RCC4-sh2 pools (D).

(E and F) RCC4 (–) and RCC4-VHL (+) cells were treated with 10 μM MG132 or vehicle (DMSO) for the last 4 hr of a 24 hr incubation at 20% O_2 (E) or at the indicated O_2 concentration (F).

these cells. PGC-1β mRNA and protein expression was also VHL dependent in RCC10 subclones (Figures S5 and S7). PGC-1β mRNA levels were increased in RCC4 subclones with loss of function for HIF-1α and/or HIF-2α (Figures 6C and 6D), consistent with regulation through the VHL/HIF-1 pathway.

PGC-1β mRNA and protein levels were increased in subclones of RCC4 and RCC4-VHL cells transduced with a vector encoding C-MYC (Figures 6A and 6B). Regulated expression of PGC-1β mRNA and protein was also observed in Epstein-Barr virus (EBV)-transformed P493 human lymphoid cells stably transfected with a tetracycline-repressible C-MYC expression vector (Figure 6E). Global mapping studies reported binding of C-MYC to the *PPARGC1B* gene encoding PGC-1β (Zeller et al., 2006). Two copies of the C-MYC binding sequence (5′-CACGTG-3′) were identified within intron 1 of *PPARGC1B*. Using primers that span these sites, tetracycline-regulated C-MYC binding to the *PPARGC1B* gene in P493 cells was demonstrated by ChIP (Figure 6F).

To demonstrate the critical role of PGC-1β as a downstream mediator of VHL and C-MYC, RCC4-VHL cells were transduced with a retroviral vector encoding shRNA against PGC-1β (Figure S14), which completely eliminated the differences between the RCC4-VHL and RCC4

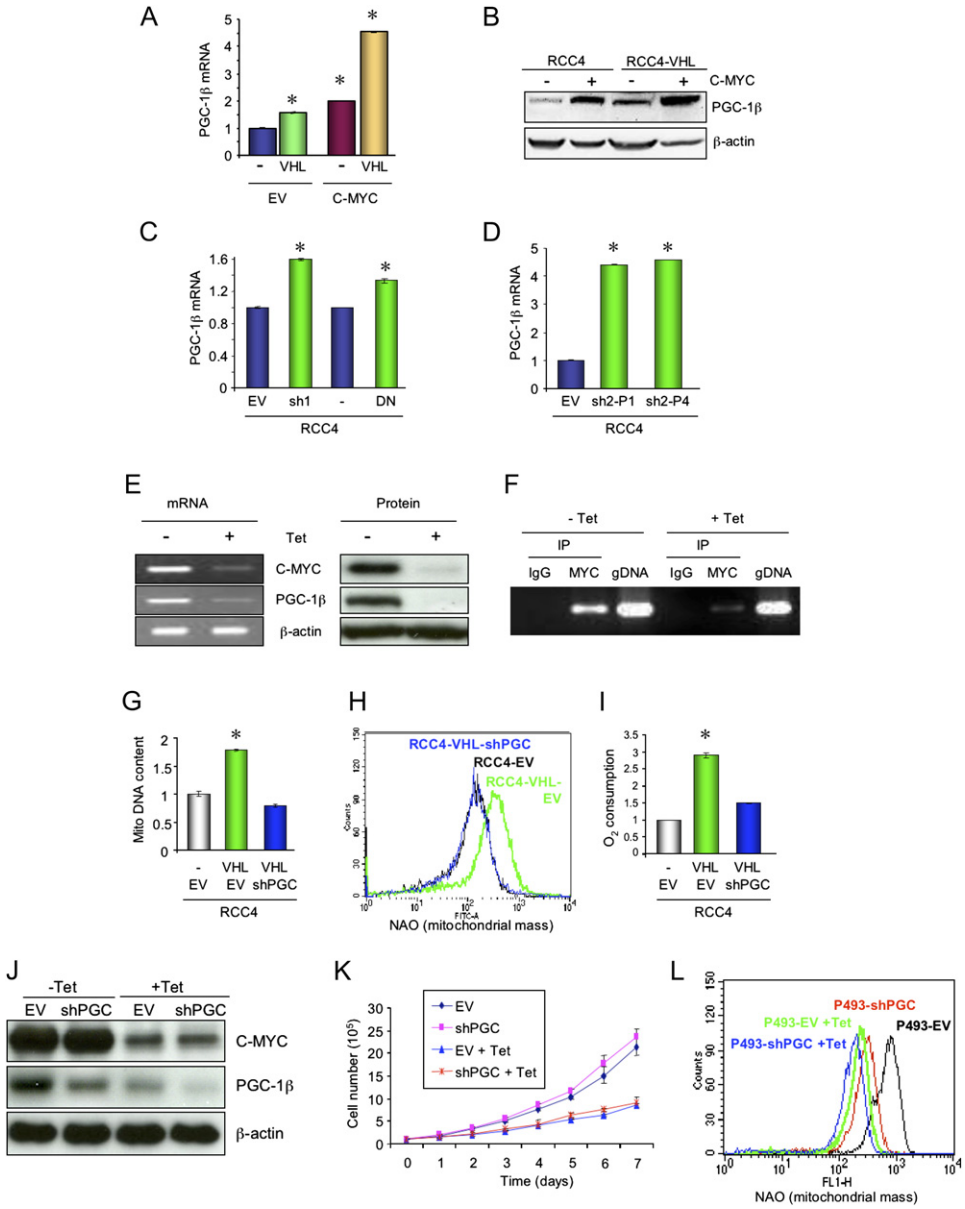

Figure 6. PGC-1β-Mediated Mitochondrial Biogenesis Is Regulated by HIF-1 and C-MYC

(A, C, and D) qrtPCR was performed for PGC-1β mRNA relative to 18S rRNA. The results for each subclone were normalized to those obtained from RCC4 cells transfected with empty vector (EV). (B) PGC-1β protein levels in RCC4 subclones were determined by immunoblot assay. (E and F) P493 cells transfected with a tetracycline (Tet)-repressible C-MYC expression vector were incubated for 72 hr in the absence (−) or presence (+) of Tet and analyzed for: C-MYC, PGC-1β, and β-actin mRNA and protein (E); and binding of C-MYC to the *PPARGC1B* promoter by ChIP (F). (G–I) Mitochondrial DNA content, mitochondrial mass, and O_2 consumption were measured in RCC4 and RCC4-VHL cells that were transfected with EV or vector encoding shRNA against PGC-1β. (J–L) P493 cells were incubated in media containing estradiol in the absence (−) or presence (+) of Tet for 72 hr and analyzed for C-MYC and PGC-1β protein expression (J), cell proliferation (K), and mitochondrial mass (L). *Mean (±SEM) that is significantly different from RCC4-EV.

subclones with regard to mitochondrial DNA, mitochondrial mass, and O_2 consumption (Figures 6G–6I). C-MYC plays an important role in cell proliferation, and downregulation of C-MYC activity may inhibit mitochondrial biogenesis indirectly through growth arrest. To rule out this possibility, we analyzed P493 cells transduced with empty vector or vector encoding shRNA against PGC-1β. The cells were grown in the presence of estradiol, which activates an EBV nuclear antigen-estrogen receptor fusion protein that is expressed from sequences engineered into the EBV genome. Estradiol treatment triggers an EBV-mediated proliferative program that induces endogenous C-MYC expression. Whereas treatment with Tet alone induces growth arrest, treatment with estradiol and

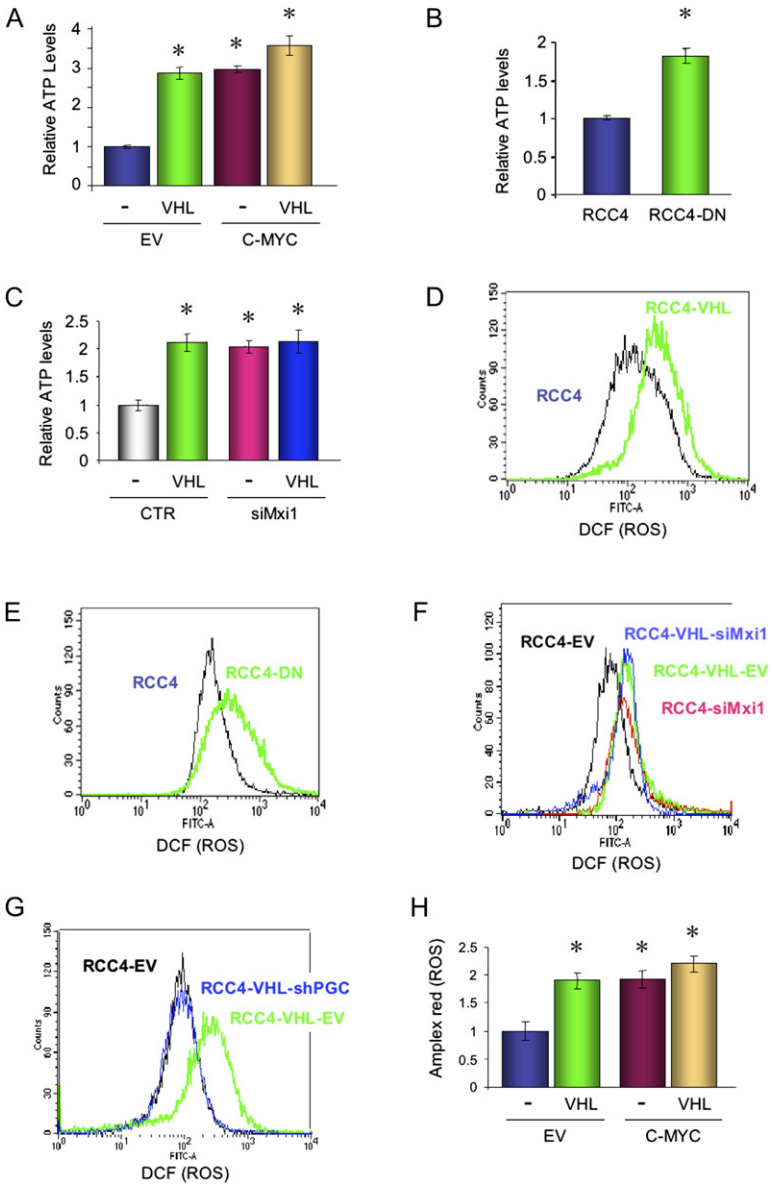

Figure 7. Analysis of ATP and Reactive Oxygen Species in RCC4 Subclones

The indicated subclones of RCC4 cells were analyzed for ATP concentration (A–C) and for ROS levels by DCF (D–G) or amplex red (H) fluorescence. *Mean (±SEM) that is significantly different from RCC4-EV or RCC4-CTR.

Tet does not induce growth arrest, allowing analysis of the effects of PGC-1β loss of function under conditions of ectopic (high) or endogenous (low) C-MYC expression in cells treated with estradiol or estradiol and Tet, respectively. Tetracycline treatment reduced C-MYC levels, cell proliferation, and mitochondrial mass, whereas PGC-1β loss of function reduced mitochondrial mass, especially in the presence of C-MYC, without a significant effect on cell proliferation (Figures 6J–6L). Taken together, the data in Figure 6 indicate that by activating *PPARGC1B* gene expression, C-MYC specifically promotes mitochondrial biogenesis.

Functional Consequences of Reduced Mitochondrial Metabolism in RCC4 Cells

We next investigated the effect of VHL loss of function on cellular energetics. The reduction in ATP levels that was observed in VHL-deficient RCC4 cells could be rescued by VHL or C-MYC gain of function (Figure 7A) and by HIF-1 (Figure 7B) or MXI-1 (Figure 7C) loss of function. ATP levels were also VHL regulated in RCC10 subclones (Figure S15A). These results indicate that the increased glucose transport and glycolysis, which occur as a result of HIF-1 gain of function in RCC4 cells, are not sufficient to compensate for the markedly reduced efficiency of glycolysis as a means of generating ATP from glucose.

Because mitochondria are the major site of ROS production, we next investigated the levels of ROS in RCC4 subclones. Cells were incubated with the nonfluorescent compound dichlorodihydrofluorescein diacetate, which in the presence of oxidants is converted to the highly fluorescent dichlorofluorescein (DCF). Flow cytometry was performed to quantify the DCF signal. Compared to RCC4 cells, RCC4-VHL (Figure 7D), RCC4-DN

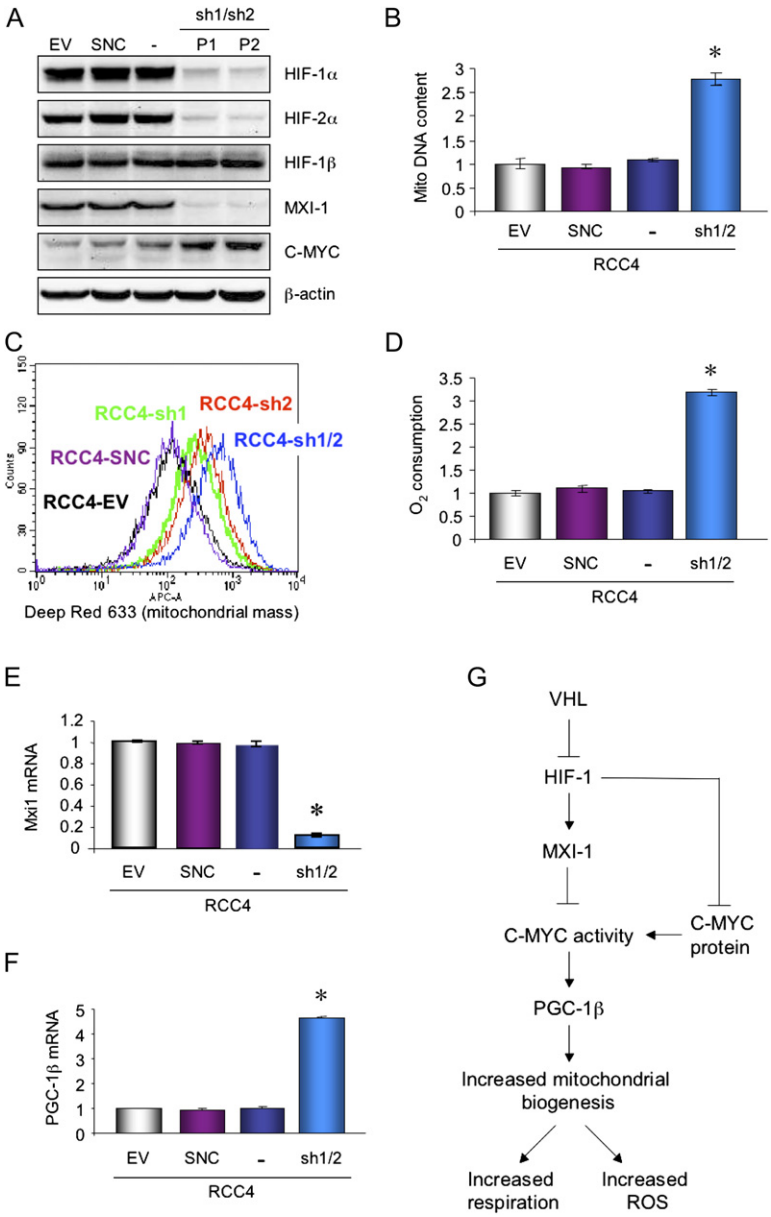

Figure 8. Analysis of Cells Lacking Both HIF-1α and HIF-2α

(A–F) Parental RCC4 cells and subclones transfected with empty vector (EV), vector encoding a scrambled negative control shRNA (SNC), or vectors encoding shRNA against HIF-1α (RCC4-sh1), HIF-2α (RCC4-sh2), or HIF-1α and HIF-2α (RCC4-sh1/2) were analyzed for protein expression (A), mitochondrial DNA (B), mitochondrial mass (C), O_2 consumption (D), and expression of MXI-1 (E) or PGC-1β (F) mRNA. *Mean (±SEM) that is significantly different from RCC4-EV.

(G) Molecular pathways regulating mitochondrial biogenesis, respiration, and ROS production in renal carcinoma cells.

(Figure 7E), and RCC4-siMxi1 (Figure 7F) cells all manifested increased levels of ROS, whereas PGC-1β loss of function led to reduced ROS levels in RCC4-VHL-shPGC cells (Figure 7G). Amplex red staining of RCC4-MYC cells revealed increased ROS production compared to RCC4-EV cells (Figure 7H). Levels of ROS were also increased in RCC10-VHL as compared to RCC10 cells (Figure S15B).

Analysis of RCC4 Subclones with Combined Loss of HIF-1α and HIF-2α

RCC4 cells were cotransduced with retroviruses encoding shRNAs against HIF-1α and HIF-2α, and two pools of cells with very low levels of both HIF-1α and HIF-2α protein were established (Figure 8). Compared to cells with knockdown of either HIF-1α or HIF-2α (Figures 2, 5, and 6), the double knockdown cells showed more dramatic increases in mitochondrial DNA, mitochondrial mass, O_2 consumption, C-MYC protein, CAD, RCL, and PGC-1β mRNA and more dramatic reductions in MXI-1 mRNA and protein levels (Figure 8; Figure S16). Taken together with the results of the single subunit knockdown experiments, these data indicate that mitochondrial mass and respiration are inversely related to the total HIF-1 activity (HIF-1α:HIF-1β and HIF-2α:HIF-1β heterodimers) in these cells. In all of these assays, the results obtained with the double knockdown cells were similar to those from RCC4-VHL cells, indicating that the combined expression of HIF-1α and HIF-2α is responsible for the loss of C-MYC and PGC-1β activity that leads to loss of mitochondrial mass and respiration in VHL-deficient renal carcinoma cells.

DISCUSSION

In this study we have delineated a molecular pathway by which glucose/energy metabolism is reprogrammed in VHL-deficient renal carcinoma cells such that mitochondrial DNA content, mitochondrial mass, cellular O_2 consumption, and ROS production are significantly reduced (Figure 8G). This pathway is triggered by loss of VHL function and the consequent dysregulated activity of HIF-1, which leads to the inhibition of C-MYC transcriptional activity by MXI-1 expression and increased C-MYC degradation by the proteasome, both of which are HIF-1 dependent. The resulting loss of C-MYC-dependent PGC-1β expression is responsible for the reduction in mitochondrial mass in VHL-deficient renal carcinoma cells. Recent studies have demonstrated that VHL positively regulates p53 activity (Roe et al., 2006) and p53 positively regulates cytochrome *c* oxidase assembly (Matoba et al., 2006). However, in RCC4 and RCC10 cells, it appears that increased HIF-1 activity resulting from VHL loss of function is sufficient to account for the repression of mitochondrial metabolism and cellular respiration.

Previous studies have demonstrated that HIF-1 transactivates genes encoding glucose transporters and glycolytic enzymes, including LDH-A, thus increasing flux through the glycolytic pathway and the conversion of pyruvate to lactate (Semenza et al., 1994, 1996; Firth et al., 1995; Iyer et al., 1998; Seagroves et al., 2001; Robey et al., 2005). Recent studies have demonstrated that HIF-1 actively shunts pyruvate away from the mitochondria by activating expression of PDK1, a kinase that inactivates pyruvate dehydrogenase and prevents the conversion of pyruvate to acetyl CoA (Kim et al., 2006; Papandreou et al., 2006). In the present study we demonstrate that mitochondrial metabolism and biogenesis are actively repressed in renal carcinoma cells with VHL loss of function and consequent HIF-1 gain of function. Taken together with previous studies, these results in VHL-deficient renal carcinoma cells provide the most detailed delineation of the molecular mechanisms underlying the triad of increased glucose uptake, increased lactate production, and decreased respiration that are the hallmarks of cancer cell metabolism.

Our studies have provided insights into the cooperative and antagonistic functional relationships between HIF-1 and C-MYC as they relate to the control of energy metabolism. Whereas HIF-1 and C-MYC both promote glucose transport and glycolysis, HIF-1 counteracts C-MYC-mediated mitochondrial biogenesis, highlighting functional differences between HIF-1, which mediates adaptive responses to low O_2, and C-MYC, which stimulates growth and proliferation. Data from the present study indicate that in renal carcinoma cells HIF-1 is upstream of C-MYC in the transcriptional network regulating oxidative and glycolytic metabolism. Previous studies demonstrated that *TFAM* is a C-MYC target gene in lymphoid cells (Li et al., 2005), but TFAM mRNA levels were not correlated with C-MYC activity or VHL status in RCC4 cells (data not shown). Instead, loss of C-MYC-dependent PGC-1β expression plays a critical role in the loss of mitochondrial mass in VHL-deficient RCC4 cells (Figure 6). Although we have focused on the consequences of VHL loss of function, MXI-1 and C-MYC expression and activity were O_2 regulated in VHL-rescued cells (Figures 4 and 5; Figure S4), suggesting that HIF-1 may mediate reduced mitochondrial biogenesis and respiration in hypoxic regions of tumors that are not VHL deficient. Although increased C-MYC degradation in hypoxic cells has been observed (Corn et al., 2005), the regulation of C-MYC protein levels by HIF-1 has not been previously reported. Additional experimentation will be required to identify domains within C-MYC that are required for degradation and to determine whether HIF-1-dependent degradation of C-MYC involves changes in posttranslational modifications or protein-protein interactions or both.

Does reprogramming cellular glucose and energy metabolism provide a selective advantage to cells with VHL loss of function? ATP levels in VHL-deficient RCC4 cells are remarkably reduced and this deficiency can be corrected by forced expression of VHL or C-MYC and by inhibition of HIF-1 or MXI-1 (Figure 7). These results indicate that under nonhypoxic conditions, VHL loss of function provides no selective advantage with respect to cellular energetics. Instead, our studies have demonstrated that decreased respiration is associated with a reduction in ROS. Preliminary studies suggest that HIF-1-dependent downregulation of mitochondrial metabolism may provide a survival benefit by reducing the risk of apoptosis (data not shown). Forced expression of HIF-1α in oral squamous cell carcinoma lines leads to reduced ROS levels and decreased hypoxia-induced apoptosis (Sasabe et al., 2005). A correlation between levels of mitochondrial respiration, ROS production, and apoptosis has been reported in several cancer cell lines (Santamaria et al., 2006). Another potentially important consequence of increased glycolysis and reduced ROS generation is inhibition of cellular senescence (Kondoh et al., 2005). Thus, proliferation and survival of renal carcinoma cells may be promoted by the reprogramming of glucose and energy metabolism that results from dysregulation of the VHL/HIF-1/C-MYC pathway. High LDH levels and low mitochondrial respiratory chain content are each associated with poor prognosis in advanced renal cell carcinoma (Simonnet et al., 2002; Motzer et al., 2004). The surprising finding that in RCC4 and RCC10 cells HIF-1 dominantly represses the activity of C-MYC, which is upregulated in many other cancers, suggests that metabolic reprogramming may be a critical step during renal cell carcinogenesis.

EXPERIMENTAL PROCEDURES

Establishment and Maintenance of Cell Lines

VHL-deficient lines RCC4 and RCC10 and subclones stably transfected with an expression vector encoding VHL and neomycin resistance were maintained in high glucose (4.5 mg/ml) DMEM with 10% fetal bovine serum (FBS) and 1% penicillin-streptomycin. RCC4-sh1 cells were described previously (Krishnamachary et al., 2006). shRNA targeting HIF-2α (nucleotides 1601–1619, GenBank NM_001430) was

inserted into pSR.retro.GFP.Neo (OligoEngine, Seattle, WA), and RCC4-sh2 pools were established by retrovirus infection and antibiotic selection. G418 (0.8 mg/ml) was added to the medium of RCC4-VHL, RCC10-VHL, RCC4-sh1, and RCC4-sh2 cells. The PGC-1β shRNA coding sequence (nucleotides 2834–2852, GenBank NM_133263) was inserted into pSuper.retro.puro (OligoEngine). RCC4-sh1/sh2 was generated by retrovirus infection (Neo-sh1/Puro-sh2) and antibiotic selection with G418 (0.8 mg/ml) and puromycin (0.8 μg/ml). RCC4-DN cells (Jiang et al., 1996) were maintained in hygromycin (400 μg/ml). Nonhypoxic cells (20% O_2) were maintained at 37°C in a 5% CO_2, 95% air incubator. Hypoxic cells (1% O_2) were maintained in a chamber flushed with a gas mixture containing 1% O_2, 5% CO_2, and 94% N_2 at 37°C. The pBabeMNiresGFP-C-Myc vector (Oster et al., 2003) or pBabeMNiresGFP empty vector (provided by Dr. L. Penn) was cotransfected with plasmids encoding group antigen/polymerase/envelope and vesicular stomatitis virus G proteins into 293T packaging cells using Fugene-6 (Roche Applied Science), and transduction was performed as described (Krishnamachary et al., 2006). P493 cells were previously described (Pajic et al., 2001).

Immunoblot Assays

Equal amounts of protein extracted from cells with RIPA buffer were fractionated by 10% SDS-PAGE. Polyclonal anti-HIF-2α antibody (Novus Biologicals), monoclonal anti-HIF-1α (H1α67; Zhong et al., 1999) and HIF-1β (H1β234; Zagzag et al., 2000) antibodies (Novus Biologicals), monoclonal anti-C-MYC antibody (9E10; Santa Cruz), and polyclonal anti-MXI-1 antibody (G-16; Santa Cruz) were used for immunoblot assays. Blots were stripped and reprobed with a polyclonal antibody against β-actin (Santa Cruz) to confirm equal protein loading and transfer.

Mitochondrial DNA Copy Measurement

Total DNA was isolated from cell lysates. The amount of mitochondrial DNA relative to nuclear genomic DNA was determined by quantitative real-time PCR using primers (listed in Table S1) for cytochrome b (mitochondrial) and RPL13A (nuclear). Relative mitochondrial DNA levels were calculated based on the threshold cycle (Ct) as $2^{-\Delta(\Delta Ct)}$, where $\Delta Ct = Ct_{Cytochrome\ b} - Ct_{RPL13A}$ and $\Delta(\Delta Ct) = \Delta Ct_{RCC4} - \Delta Ct_{subclone}$.

Flow Cytometry

Mitochondrial mass and intracellular ROS production were measured by staining cells with 10 nM NAO or 25 nM deep red 633 and 1 μM dichlorodihydrofluorescein diacetate (Molecular Probes), respectively, at 37°C for 15 min in PBS containing 5% FBS. Stained cells were filtered and analyzed immediately in a FACScan flow cytometer (BD Bioscience). Gain and amplifier settings were held constant during the experiment.

Measurement of Total Cellular O_2 Consumption

Cells were trypsinized and suspended at 3–8 × 10^6 per ml in DMEM medium with 10% FBS and 25 mM HEPES buffer. For each experiment, equal numbers of cells suspended in 0.4 ml were pipetted into the chamber of an Oxytherm electrode unit (Hansatech Instrument Ltd.), which uses a Clark-type electrode to monitor the dissolved oxygen concentration in the sealed chamber over time. The data were exported to a computerized chart recorder (Oxygraph, Hansatech Instrument Ltd.), which calculated the rate of O_2 consumption. The temperature was maintained at 37°C during the measurement. The O_2 concentration in 0.4 ml of DMEM medium without cells was also measured over time to provide background values. Relative O_2 consumption rate was calculated after correcting for background.

Measurement of Electron Transport Complex III Activity

Ubiquinol-ferricytochrome c oxido-reductase activity of mitochondria isolated from 3 × 10^6 cells was measured in the presence and absence of antimycin A (10 μg/ml) as previously described (Yuan et al., 2003) and the antimycin-inhibited activity was expressed as nmol of cytochrome c reduced per min.

qrtPCR

RNA was isolated using Trizol (Invitrogen) followed by DNase (Ambion) treatment. Primers were designed using Beacon Designer software, and cDNA was prepared using the iScript cDNA synthesis kit (Bio-Rad). cDNA samples were diluted 1:10, and real-time PCR was performed using iQ SYBR Green Supermix and the iCycler Real-time PCR Detection System (Bio-Rad). For each primer pair (Table S1), annealing temperature was optimized by gradient PCR. The fold change in expression of each target mRNA relative to 18S rRNA was calculated as $2^{-\Delta(\Delta Ct)}$, where $\Delta Ct = Ct_{target} - Ct_{18S}$ and $\Delta(\Delta Ct) = \Delta Ct_{RCC4} - \Delta Ct_{subclone}$.

siRNA Transfection

siRNAs targeting human C-MYC or MXI-1 mRNA (siGENOME SMART pools M-003282-04 and M-009947-00, Dharmacon Research Inc.) or RISC-free control siRNA (Dharmacon) were transfected into RCC4 subclones in the presence of Oligofectamine (Invitrogen). After 72 hr, cells were harvested.

Reporter Gene Assay

A 53-bp sequence from human *MXI1* gene was amplified by PCR and inserted into the *Bgl* II site of pGL2-Promoter (Promega). HEK293 cells (4 × 10^4 per well) were seeded in a 48-well plate. After overnight incubation, cells were transfected either with 100 ng of firefly luciferase reporter plasmid and 4 ng of pSV-*Renilla* plasmid, or further cotransfected with expression vector encoding Flag-HIF-1α or HIF-2α. The total amount of DNA transfected per well was held constant by addition of empty vector. Eighteen hours after transfection, cells were incubated at 1% or 20% O_2 for 24 hr. Luciferase activities were measured using the Dual-Luciferase Reporter Assay System (Promega). For each experiment, at least two independent transfections in triplicate were performed.

ChIP Assay

ChIP was performed with the ChIP assay kit from Upstate-Cell Signaling Solutions (Temecula, CA) with rabbit polyclonal antibodies against HIF-1α, HIF-2α, or C-MYC (Santa Cruz Biotechnology).

Intracellular ATP

ATP levels were measured using an ATP assay kit (Sigma) according to the manufacturer's instructions. Luminescence was measured using a Wallace microplate luminescence reader (Perkin Elmer) and normalized to the protein concentration.

Supplemental Data

The Supplemental Data include 16 supplemental figures and one supplemental table and can be found with this article online at http://www.cancercell.org/cgi/content/full/11/5/407/DC1/.

ACKNOWLEDGMENTS

We thank Celeste Simon and Miguel Esteban for providing RCC4-VHL and RCC10-VHL cell lines, respectively; Joseph Garcia for providing HIF-2α expression vector; Bruce Spiegelman and Pere Puigserver for anti-PGC-1β antibodies; Karen Padgett and Novus Biologicals for anti-HIF-2α antibodies; Linda Penn for providing pBabeMNiresGFP-C-Myc retroviral vector; and Linzhao Cheng for providing advice and reagents for retrovirus production. This work was supported in part by PHS grants P50-CA103175 and R37-CA51497 from the NIH.

Received: June 26, 2006
Revised: January 22, 2007
Accepted: April 2, 2007
Published: May 7, 2007

REFERENCES

Bogacka, I., Xie, H., Bray, G.A., and Smith, S.R. (2005). Pioglitazone induces mitochondrial biogenesis in human subcutaneous adipose tissue in vivo. Diabetes *54*, 1392–1399.

Boyd, K.E., and Farnham, P.J. (1997). Myc versus USF: Discrimination at the cad gene is determined by core promoter elements. Mol. Cell. Biol. *17*, 2529–2537.

Brizel, D.M., Schroeder, T., Scher, R.L., Walenta, S., Clough, R.W., Dewhirst, M.W., and Mueller-Klieser, W. (2001). Elevated tumor lactate concentrations predict for an increased risk of metastases in head-and-neck cancer. Int. J. Radiat. Oncol. Biol. Phys. *51*, 349–353.

Carroll, R.C., Ash, R.F., Vogt, P.K., and Singer, S.J. (1978). Reversion of transformed glycolysis to normal by inhibition of protein synthesis in rat kidney cells infected with temperature-sensitive mutant of Rous sarcoma virus. Proc. Natl. Acad. Sci. USA *75*, 5015–5019.

Corn, P.G., Ricci, M.S., Scata, K.A., Arsham, A.M., Simon, M.C., Dicker, D.T., and El-Deiry, W.S. (2005). Mxi1 is induced by hypoxia in a HIF-1-dependent manner and protects cells from c-Myc-induced apoptosis. Cancer Biol. Ther. *4*, 1285–1294.

Craven, R.A., Hanrahan, S., Totty, N., Harnden, P., Stanley, A.J., Maher, E.R., Harris, A.L., Trimble, W.S., Selby, P.J., and Banks, R.E. (2006). Proteomic identification of a role for the von Hippel Lindau tumour suppressor in changes in the expression of mitochondrial proteins and septin 2 in renal cell carcinoma. Proteomics *6*, 3880–3893.

Cuezva, J.M., Chen, G., Alonso, A.M., Isidoro, A., Misek, D.E., Hanash, S.M., and Beer, D.G. (2004). The bioenergetic signature of lung adenocarcinomas is a molecular marker of cancer diagnosis and prognosis. Carcinogenesis *25*, 1157–1163.

Cuezva, J.M., Krajewska, M., Lopez de Heredia, M., Krajewski, S., Santamaria, G., Kim, H., Zapata, J.M., Marusawa, H., Chamorrow, M., and Reed, J.C. (2002). The bioenergetic signature of cancer: A marker of tumor progression. Cancer Res. *62*, 6674–6681.

Discher, D.J., Bishopric, N.H., Wu, X., Peterson, C.A., and Webster, K.A. (1998). Hypoxia regulates beta-enolase and pyruvate kinase-M promoters by modulating Sp1/Sp3 binding to a conserved GC element. J. Biol. Chem. *273*, 26087–26093.

Elstrom, R.L., Bauer, D.E., Buzzai, M., Karnauskas, R., Harris, M.H., Plas, D.R., Zhuang, H., Cinalli, R.M., Alavi, A., Rudin, C.M., and Thompson, C.B. (2004). Akt stimulates aerobic glycolysis in cancer cells. Cancer Res. *64*, 3892–3899.

Esteban, M.A., Tran, M.G., Harten, S.K., Hill, P., Castellanos, M.C., Chandra, A., Raval, R., O'Brien, T.S., and Maxwell, P.H. (2006). Regulation of E-cadherin expression by VHL and hypoxia-inducible factor. Cancer Res. *66*, 3567–3575.

Fantin, V.R., St-Pierre, J., and Leder, P. (2006). Attenuation of LDH-A expression uncovers a link between glycolysis, mitochondrial physiology, and tumor maintenance. Cancer Cell *9*, 425–434.

Firth, J.D., Ebert, B.L., and Ratcliffe, P.J. (1995). Hypoxic regulation of lactate dehydrogenase A: Interaction between hypoxia-inducible factor 1 and cAMP response elements. J. Biol. Chem. *270*, 21021–21027.

Garcia, J.A. (2006). HIFing the brakes: Therapeutic opportunities for treatment of human malignancies. Sci. STKE. *30*, pe25.

Gatenby, R.A., and Gillies, R.J. (2004). Why do cancers have high aerobic glycolysis? Nat. Rev. Cancer *4*, 891–899.

Hervouet, E., Demont, J., Pecina, P., Vojtiskova, A., Houstek, J., Simonnet, H., and Godinot, C. (2005). A new role for the von Hippel-Lindau tumor suppressor protein: Stimulation of mitochondrial oxidative phosphorylation complex biogenesis. Carcinogenesis *26*, 531–539.

Hervouet, E., and Godinot, C. (2006). Mitochondrial disorders in renal tumors. Mitochondrion *6*, 105–117.

Hu, C.J., Wang, L.Y., Chodosh, L.A., Keith, B., and Simon, M.C. (2003). Differential roles of hypoxia-inducible factor 1α (HIF-1α) and HIF-2α in hypoxic gene regulation. Mol. Cell. Biol. *23*, 9361–9374.

Iyer, N.V., Kotch, L.E., Agani, F., Leung, S.W., Laughner, E., Wenger, R.H., Gassmann, M., Gearhart, J.D., Lawler, A.M., Yu, A.Y., and Semenza, G.L. (1998). Cellular and developmental control of O_2 homeostasis by hypoxia-inducible factor 1α. Genes Dev. *12*, 149–162.

Jiang, B.-H., Agani, F., Passaniti, A., and Semenza, G.L. (1997). V-SRC induces expression of hypoxia-inducible factor 1 (HIF-1) and transcription of genes encoding vascular endothelial growth factor and enolase 1: Involvement of HIF-1 in tumor progression. Cancer Res. *57*, 5328–5335.

Jiang, B.H., Rue, E., Wang, G.L., Roe, R., and Semenza, G.L. (1996). Dimerization, DNA binding, and transactivation properties of hypoxia-inducible factor 1. J. Biol. Chem. *271*, 17771–17778.

Kelly, D.P., and Scarpulla, R.C. (2004). Transcriptional regulatory circuits controlling mitochondrial biogenesis and function. Genes Dev. *18*, 357–368.

Kim, J.-w., Tchernyshyov, I., Semenza, G.L., and Dang, C.V. (2006). HIF-1-mediated expression of pyruvate dehydrogenase kinase: A metabolic switch required for cellular adaptation to hypoxia. Cell Metab. *3*, 177–185.

Kondo, K., Klco, J., Nakamura, E., Lechpammer, M., and Kaelin, W.G., Jr. (2002). Inhibition of HIF is necessary for tumor suppression by the von Hippel-Lindau protein. Cancer Cell *1*, 237–246.

Kondoh, H., Lleonart, M.E., Gil, J., Wang, J., Degan, P., Peters, G., Martinez, D., Carnero, A., and Beach, D. (2005). Glycolytic enzymes can modulate cellular life span. Cancer Res. *65*, 177–185.

Krieg, M., Haas, R., Brauch, H., Acker, T., Flamme, I., and Plate, K.H. (2000). Up-regulation of hypoxia-inducible factors HIF-1α and HIF-2α under normoxic conditions in renal carcinoma cells by von Hippel-Lindau tumor suppressor gene loss of function. Oncogene *19*, 5435–5443.

Krishnamachary, B., Zagzag, D., Nagasawa, H., Rainey, K., Okuyama, H., Baek, J.H., and Semenza, G.L. (2006). Hypoxia-inducible factor-1-dependent repression of E-cadherin in von Hippel-Lindau tumor suppressor-null renal cell carcinoma mediated by TCF3, ZFHX1A, and ZFHX1B. Cancer Res. *66*, 2725–2731.

Lewis, B.C., Shim, H., Li, Q., Wu, C.S., Lee, L.A., Maity, A., and Dang, C.V. (1997). Identification of putative c-Myc-responsive genes: Characterization of rcl, a novel growth-related gene. Mol. Cell. Biol. *17*, 4967–4978.

Li, F., Wang, Y., Zeller, K.I., Potter, J.J., Wonsey, D.R., O'Donnell, K.A., Kim, J.-w., Yustein, J.T., Lee, L.A., and Dang, C.V. (2005). Myc stimulates nuclearly encoded mitochondrial genes and mitochondrial biogenesis. Mol. Cell. Biol. *25*, 6225–6234.

Manalo, D.J., Rowan, A., Lavoie, T., Natarajan, L., Kelly, B.D., Ye, S.Q., Garcia, J.G., and Semenza, G.L. (2005). Transcriptional regulation of vascular endothelial cell responses to hypoxia by HIF-1. Blood *105*, 659–669.

Mandriota, S.J., Turner, K.J., Davies, D.R., Murray, P.G., Morgan, N.V., Sowter, H.M., Wykoff, C.C., Maher, E.R., Harris, A.L., Ratcliffe, P.J., and Maxwell, P.H. (2002). HIF activation identifies early lesions in VHL kidneys: Evidence for site-specific tumor suppressor function in the nephron. Cancer Cell *1*, 459–468.

Maranchie, J.K., Vasselli, J.R., Riss, J., Bonifacino, J.S., Linehan, W.M., and Klausner, R.D. (2002). The contribution of VHL substrate binding and HIF-1α to the phenotype of VHL loss in renal cell carcinoma. Cancer Cell *1*, 247–255.

Matoba, S., Kang, J.-G., Patino, W.D., Wragg, A., Boehm, M., Gavrilova, O., Hurley, P.J., Bunz, F., and Hwang, P.M. (2006). p53 regulates mitochondrial respiration. Science *312*, 1650–1653.

Maxwell, P.H., Wiesener, M.S., Chang, G.W., Clifford, S.C., Vaux, E.C., Cockman, M.E., Wykoff, C.C., Pugh, C.W., Maher, E.R., and Ratcliffe, P.J. (1999). The tumor suppressor protein VHL targets hypoxia-inducible factors for oxygen-dependent proteolysis. Nature *399*, 271–275.

Meierhofer, D., Mayr, J.A., Foetschl, U., Berger, A., Fink, K., Schmeller, N., Hacker, G.W., Hauser-Kronberger, C., Kofler, B., and Sperl, W. (2004). Decrease of mitochondrial DNA content and energy metabolism in renal cell carcinoma. Carcinogenesis *25*, 1005–1010.

Melillo, G. (2006). Inhibiting hypoxia-inducible factor 1 for cancer therapy. Mol. Cancer Res. *4*, 601–605.

Moeller, B.J., Dreher, M.R., Rabbani, Z.N., Schroeder, T., Cao, Y., Li, C.Y., and Dewhirst, M.W. (2005). Pleiotropic effects of HIF-1 blockade on tumor radiosensitivity. Cancer Cell *8*, 99–110.

Motzer, R.J., Bacik, J., and Mazumdar, M. (2004). Prognostic factors for survival of patients with stage IV renal cell carcinoma: Memorial Sloan-Kettering Cancer Center experience. Clin. Cancer Res. *10*, 6302S–6303S.

Oster, S.K., Mao, D.Y., Kennedy, J., and Penn, L.Z. (2003). Functional analysis of the N-terminal domain of the Myc oncoprotein. Oncogene *22*, 1998–2010.

Osthus, R.C., Shim, H., Kim, S., Li, Q., Reddy, R., Mukherjee, M., Xu, Y., Wonsey, D., Lee, L.A., and Dang, C.V. (2000). Deregulation of glucose transporter 1 and glycolytic gene expression by c-Myc. J. Biol. Chem. *275*, 21797–21800.

Pajic, A., Staege, M.S., Dudziak, D., Schuhmacher, M., Spitkovsky, D., Eissner, G., Brielmeier, M., Polack, A., and Bornkamm, G.W. (2001). Antagonistic effects of c-myc and Epstein-Barr virus latent genes on the phenotype of human B cells. Int. J. Cancer *93*, 810–816.

Papandreou, I., Cairns, R.A., Fontana, L., Lim, A.L., and Denko, N.C. (2006). HIF-1 mediates adaptation to hypoxia by actively downregulating mitochondrial oxygen consumption. Cell Metab. *3*, 187–197.

Petros, J.A., Baumann, A.K., Ruiz-Pesini, E., Amin, M.B., Sun, C.Q., Hall, J., Lim, S., Issa, M.M., Flanders, W.D., Hosseini, S.H., et al. (2005). mtDNA mutations increase tumorigenicity in prostate cancer. Proc. Natl. Acad. Sci. USA *102*, 719–724.

Polyak, K., Li, Y., Zhu, H., Lengauer, C., Willson, J.K., Markowitz, S.D., Trush, M.A., Kinzler, K.W., and Vogelstein, B. (1998). Somatic mutations of the mitochondrial genome in human colorectal tumors. Nat. Genet. *20*, 291–293.

Raval, R.R., Lau, K.W., Tran, M.G., Sowter, H.M., Mandriota, S.J., Li, J.L., Pugh, C.W., Maxwell, P.H., Harris, A.L., and Ratcliffe, P.J. (2005). Contrasting properties of hypoxia-inducible factor 1 (HIF-1) and HIF-2 in von Hippel-Lindau-associated renal cell carcinoma. Mol. Cell. Biol. *25*, 5675–5686.

Robey, I.F., Lien, A.D., Welsh, S.J., Baggett, B.K., and Gillies, R.J. (2005). Hypoxia-inducible factor-1α and the glycolytic phenotype in tumors. Neoplasia *7*, 324–330.

Roe, J.S., Kim, H., Lee, S.M., Kim, S.T., Cho, E.J., and Youn, H.D. (2006). p53 stabilization and transactivation by von Hippel-Lindau protein. Mol. Cell *22*, 395–405.

Santamaria, G., Martinez-Diez, M., Fabregat, I., and Cuezva, J.M. (2006). Efficient execution of cell death in non-glycolytic cells requires the generation of ROS controlled by the activity of mitochondrial H^+-ATP synthase. Carcinogenesis *27*, 925–935.

Sasabe, E., Tatemoto, Y., Li, D., Yamamoto, T., and Osaki, T. (2005). Mechanism of HIF-1α-dependent suppression of hypoxia-induced apoptosis in squamous cell carcinoma cells. Cancer Sci. *96*, 394–402.

Seagroves, T.N., Ryan, H.E., Lu, H., Wouters, B.G., Knapp, M., Thibault, P., Laderoute, K., and Johnson, R.S. (2001). Transcription factor HIF-1 is a necessary mediator of the Pasteur effect in mammalian cells. Mol. Cell. Biol. *21*, 3436–3444.

Semenza, G.L. (2003). Targeting HIF-1 for cancer therapy. Nat. Rev. Cancer *3*, 721–732.

Semenza, G.L., Jiang, B.H., Leung, S.W., Passantino, R., Concordet, J.P., Maire, P., and Giallongo, A. (1996). Hypoxia response elements in the aldolase A, enolase *1*, and lactate dehydrogenase A gene promoters contain essential binding sites for hypoxia-inducible factor 1. J. Biol. Chem. *271*, 32529–32537.

Semenza, G.L., Roth, P.H., Fang, H.M., and Wang, G.L. (1994). Transcriptional regulation of genes encoding glycolytic enzymes by hypoxia-inducible factor 1. J. Biol. Chem. *269*, 23757–23763.

Shim, H., Dolde, C., Lewis, B.C., Wu, C.S., Dang, G., Jungmann, R.A., Dalla-Favera, R., and Dang, C.V. (1997). c-Myc transactivation of LDH-A: Implications for tumor metabolism and growth. Proc. Natl. Acad. Sci. USA *94*, 6658–6663.

Simonnet, H., Alazard, N., Pfeiffer, K., Gallou, C., Beroud, C., Demont, J., Bouvier, R., Schagger, H., and Godinot, C. (2002). Low mitochondrial respiratory chain content correlates with tumor aggressiveness in renal cell carcinoma. Carcinogenesis *23*, 759–768.

Tang, N., Wang, L., Esko, J., Giordano, F.J., Huang, Y., Gerber, H.-P., Ferrara, N., and Johnson, R.S. (2004). Loss of HIF-1α in endothelial cells disrupts a hypoxia-driven VEGF autocrine loop necessary for tumorigenesis. Cancer Cell *6*, 485–495.

Thomas, G.V., Tran, C., Mellinghoff, I.K., Welsbie, D.S., Chan, E., Fueger, B., Czernin, J., and Sawyers, C.L. (2006). Hypoxia-inducible factor determines sensitivity to inhibitors of mTOR in kidney cancer. Nat. Med. *12*, 122–127. Published online December 11, 2005. 10.1038/nm1337.

Tian, H., McKnight, S.L., and Russell, D.W. (1997). Endothelial PAS domain protein 1 (EPAS1), a transcription factor selectively expressed in endothelial cells. Genes Dev. *11*, 72–82.

Uldry, M., Yang, W., St-Pierre, J., Lin, J., Seale, P., and Spiegelman, B.M. (2006). Complementary action of the PGC-1 coactivators in mitochondrial biogenesis and brown fat differentiation. Cell Metab. *3*, 333–341.

Unwin, R.D., Craven, R.A., Harnden, P., Hanrahan, S., Totty, N., Knowles, M., Eardley, I., Selby, P.J., and Banks, R.E. (2003). Proteomic changes in renal cancer and co-ordinate demonstration of both the glycolytic and mitochondrial aspects of the Warburg effect. Proteomics *3*, 1620–1632.

Wang, G.L., Jiang, B.-H., Rue, E.A., and Semenza, G.L. (1995). Hypoxia-inducible factor 1 is a basic-helix-loop-helix-PAS heterodimer regulated by cellular O_2 tension. Proc. Natl. Acad. Sci. USA *92*, 5510–5514.

Warburg, O. (1930). The Metabolism of Tumours (London: Arnold Constable).

Yuan, G., Adhikary, G., McCormick, A.A., Holcroft, J.J., Kumar, G.K., and Prabhakar, N.R. (2003). Role of oxidative stress in intermittent hypoxia-induced immediate early gene activation in rat PC12 cells. J. Physiol. *557*, 773–783.

Zagzag, D., Zhong, H., Scalzitti, J.M., Laughner, E., Simons, J.W., and Semenza, G.L. (2000). Expression of hypoxia-inducible factor 1α in brain tumors: Association with angiogenesis, invasion, and progression. Cancer *88*, 2606–2618.

Zeller, K.I., Zhao, X.D., Lee, C.W.H., Chiu, K.P., Yao, F., Yustein, J.T., Ooi, H.S., Orlov, Y.L., Shahab, A., Yong, H.C., et al. (2006). Global mapping of c-myc binding sites and target gene networks in human B cells. Proc. Natl. Acad. Sci. USA *103*, 17834–17839.

Zhong, H., De Marzo, A.M., Laughner, E., Lim, M., Hilton, D.A., Zagzag, D., Buechler, P., Isaacs, W.B., Semenza, G.L., and Simons, J.W. (1999). Overexpression of hypoxia-inducible factor 1α in common human cancers and their metastases. Cancer Res. *59*, 5830–5835.